American Journal of Electrical Power and Energy Systems
2015; 4(3-1): 1-5
Published online January 16, 2015 (http://www.sciencepublishinggroup.com/j/epes)
doi: 10.11648/j.epes.s.2015040301.11
ISSN: 2326-912X (Print); ISSN: 2326-9200 (Online)

Design and optimization of axial flux brushless DC generator dedicated to generation of renewable energy

Souhir Tounsi

National School of Electronics and Telecommunications of Sfax, Sfax University, SETIT Research Unit, Sfax, Tunisia

Email address:
souhir.tounsi@isecs.rnu.tn

To cite this article:
Souhir Tounsi. Design and Optimization of Axial Flux Brushless DC Generator Dedicated to Generation of Renewable Energy. *American Journal of Electrical Power and Energy Systems.* Special Issue: Design and Monitoring of Renewable Energy Systems (DMRES). Vol. 4, No. 3-1, 2015, pp. 1-5. doi: 10.11648/j.epes.s.2015040301.11

Abstract: In this paper, we present a design model of permanent magnet generator dedicated to generate renewable energy, taking in account of several systemic and physical constraints. Being couple to a model of the losses of the power chain and to a model of the mass of the generator, this analytic model puts a problem of conjoined optimization of the recovered energy and the cost of the generator. This problem is solved by genetic algorithms method.

Keywords: Renewable Energy, Design, Generator, Converters, Optimization

1. Introduction

A modular axial generator structure with permanent magnet reducing the cost of manufacture is chosen to generate renewable energy [1], [2], [3], [4] and [5].

We choice the analytic method to conceive the permanent magnet generator seen its compatibility to optimization approaches. Indeed, it's fast and product results quickly and without iterations.

The coupling of power chain losses model and the model of the generator mass to the program dimensioning the generator, pose an optimization problem. This last is solved by the software of optimization based on the Genetic Algorithm method.

2. Renewable Energy System

The system generating renewable energy comprises:

- A propeller attached to the rotor transmitting the mechanical energy caused by the movement of the air to the stator.
- A synchronous generator with permanents magnets to convert mechanical energy from the rotor in an alternating electrical energy.
- AC-DC converter to convert the alternative energy into continuous energy.
- DC-DC converter to elevate voltage loading batteries to optimize the recovered energy.
- An energy accumulator for energy storage.

3. Structures of the Electric Generator

3.1. Manufacturing Cost Reduction

The electric generator structure is modular i.e. it can be with several stages. This technology allows the reduction of the production cost of these generators types. The slots are right and open what facilitates the coils insertion and reduces the generator manufacturing cost. The concentrated winding is used because of its advantages:

- Reduction of the manufacturing time of this generator (insertion of coils in one block).
- Reduction of the end-windings.
- Reduction of the generator bulk.

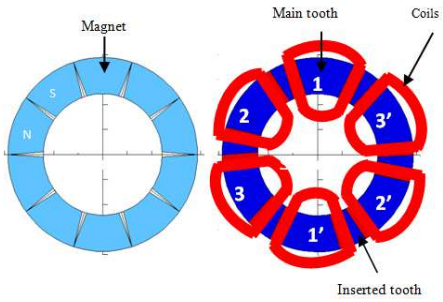

Figure 1. *5 pairs of poles, 6 main teeth, axial flux and trapezoidal configuration.*

Figure 1 illustrates the first trapezoidal configuration (n=1) with axial flux only one stage [6].

Five configurations with a trapezoidal wave-form are found while being based on optimization rules of the ripple torque and cost. Each configuration is characterized by a variation law of the pole pairs number (p) according to an integer number n varying from one to infinity, the ratio (r) of the number of main teeth (N_t) by the number of pole pairs, the ratio (ν) between the angular width between two main teeth and that of a principal tooth, the ratio (α) between the angular width of a principal tooth and that of a magnet and the ratio (β) between the angular width of a magnet and the polar step. Table .1 gives these ratios for these configurations [6], [7], [8], [9].

Table 1. *Found configurations.*

Trapezoidal configurations	p	r	ν	α	β
1	2.n	1.5	1/3	1	1
2	5.n	1.2	2/3	1	1
3	7.n	6/7	4/3	1	1
4	4.n	0.75	5/3	1	1
5	5.n	0.6	7/3	1	1

3.2. Design Methodology

We choose the analytic modelling of the generator, because it's compatible to the optimizations approaches [10], [11], [12], [13].

The worksheet computes the geometrical dimensions of rotor and stator as well as windings, temperature, inductance, leakages and efficiency for different operating points.

A sizing program is developed with equations detailed below. The program inputs are:

1. Generator specifications.
2. Materials properties.
3. Configuration, i.e. magnet number and teeth number.
4. Inner and outer diameter of the motor.
5. Notebook data.
6. Current density in coils δ.
7. Rotor yoke B_{ry}, stator yoke B_{sy}, flux density in the air-gap B_g and number of phase turn N_s.

When inputs 3. and 4. are set, magnet shapes, teeth and slots are fixed. Then, the area of one tooth A_t and the average length of a spire L_{sp} are calculated from geometric equations.

This model is validated by finite elements method. Indeed, the generator is drawn according to its geometrical magnitudes extracted from analytical model with the software Maxwell-2d, and is simulated in dynamic and static in order to compare the results obtained with those found by the analytical method.

The coupling of this model to a model evaluating the power train losses and generator mass, poses an optimization problem with several variables and constraints. This latter is solved by the genetic algorithms (GAs) method [10], [11], [12], [13].

4. Dimensioning Torque

The generator constant is defined by [10], [11], [12], [13]:

$$K_e = 2 \times N_s \times A \times B \times B_g \quad (1)$$

For the axial flux structures A and B are given by:

$$A = \frac{D_e - D_i}{2} \quad (2)$$

$$B = \frac{D_e + D_i}{2} \quad (3)$$

The dimensioning torque is given by the following relation:

$$T_{dim} = \frac{1.137 \times r \times v_{max}^3}{\Omega_{max}} \quad (4)$$

where V_{max} is the maximum air velocity, r is the radius of the rotor and Ω_{max} is the maximum angular speed of the generator.

The dimensioning current is expressed as follows:

$$I_{dim} = \frac{T_{dim}}{2 \times N_s \times A \times B \times B_g} \quad (5)$$

5. Generator Sizing

The air-gap flux density is calculated for a maximal recovery position, or the magnet is in front of a main tooth. At this position the air-gap flux density is maximal. The distribution of the field lines to the level of a pole is illustrated by the figure 2:

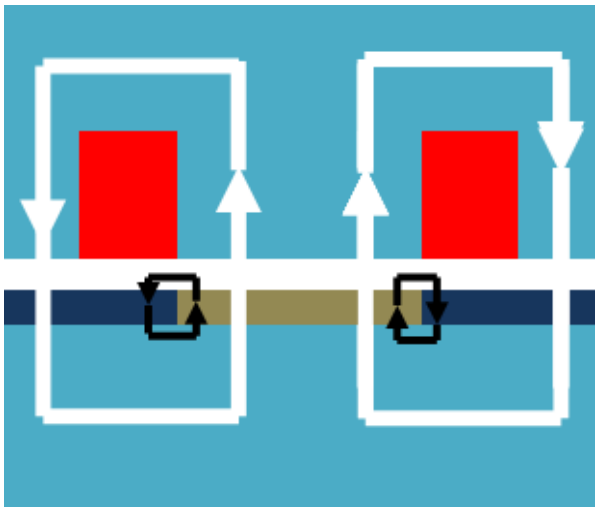

Figure 2. *Flux lines distribution at maximal recovery position.*

The flux decomposes itself in main flux and in leakages flux between magnets.

As applying the Ampere theorem to the level of a stator pole, we can deduct the flux density due to the stator current.

$$\int_{\text{flux lines}} \vec{H} \times \vec{dl} = \frac{N_s}{2} \times I_{max} = 2 \times \left(H_{ri} \times t_m + H_{ri} \times g \right) \quad (6)$$

where I_{max} is the stator maximal current, H is the magnetic

field, H_{ri} is the air-gap magnetic field, t_m is the magnet thickness and μ_0 is the air permeability.

$$B_{ri} = \mu_0 \times H_{ri} \quad (7)$$

where B_{ri} is the flux density in the air-gap due to the stator current.

$$Bri = \frac{\mu_0}{4} \times \frac{N_s \times I_{max}}{t_m + g} \quad (8)$$

While applying the Ampere theorem, we can deduct the magnet thickness imposing a fixed flux density in the different zones of the motor while disregarding the flux density due to the stator current circulation, since the flux must cross two times the air-gap thickness and magnet with permeability very close to the air permeability.

$$\int_{\text{flux lines}} \vec{H} \times \vec{dl} = 0 = 2 \times \left(H_m \times t_m + H_g \times g \right) \quad (9)$$

The air-gap flux density is linear according to the magnetic field for this working regime:

$$B_g = \mu_0 \times H_g \quad (10)$$

While applying the flux conservation theorem to the level of the air-gap, we deduct the value of the air-gap flux density in function of the magnet flux density and the coefficient of the leakages flux.

$$B_m \times S_m \times K_{fu} = B_g \times S_m \quad (11)$$

The magnet flux density becomes:

$$B_m = \frac{B_g}{K_{fu}} \quad (12)$$

The magnet flux density is approached by the following linear equation:

$$B_m = \mu_0 \times \mu_m \times H_m + B_r \quad (13)$$

where μ_m is the magnet's relative permeability, B_r is the remanence.

From the equation (10), (11), (12) and (13), we deduct the magnet thickness fixing the air-gap flux density equal to B_g:

$$t_m = \mu_m \times \frac{B_g}{B_r - \frac{B_g}{K_{fu}}} \times g \quad (14)$$

where $K_{fu} < 1$ is the magnet's leakage coefficient and g is the air-gap thickness. To avoid demagnetization, the phase currents must be lower then the demagnetization current I_d [8]:

$$I_d = \left(\frac{B_r - B_{min}}{\mu_m} \times t_m - B_{min} \times K_{fu} \times g \right) \times \frac{p}{2 \times \mu_0 \times N_s} \quad (15)$$

where Bmin is the minimum flux density allowed in the magnets and μ0 is the air permeability. The rotor yoke thickness try and stator yoke thickness tsy derive from the flux conservation [9]:

$$t_{ry} = \frac{B_g}{B_{ry}} \times \frac{\text{Min}(A_t, A_m)}{2 \times A} \times \frac{1}{K_{fu}} \quad (16)$$

$$t_{sy} = \frac{B_g}{B_{sy}} \times \frac{\text{Min}(A_t, A_m)}{2 \times A} \quad (17)$$

where A_t is the tooth area, A_m is the area of one magnet, B_{ry} and B_{sy} are respectively the flux densities in rotor and stator yokes. For the axial flux and trapezoidal wave-form motor configurations the slot height is [9]:

$$h_s = \frac{3.2.N_s}{2 N_t} \frac{I_{dim}}{\delta} \frac{1}{K_f} \frac{1}{A_s} \quad (18)$$

where N_t is the number of principal teeth, δ is the current density in slots, K_f is the slot filling factor, A_s is the slot width and I_{dim} is the dimensioning current:

$$I_{dim} = \frac{T_{dim}}{K_e} \quad (19)$$

The slot width is expressed as follows:

$$A_s = B \times \text{SIN}\left(\frac{1}{2} \times \left(\frac{2 \times \pi}{N_t} - \alpha \times \beta \times \frac{\pi}{p} \times (1 - r_{did}) \right) \right) \quad (20)$$

where r_{did} is the ratio between the angular width of the inserted tooth and that of the principal tooth. This ratio is optimized by finite elements simulations in order to reduce the flux leakages and to improve the electromotive force wave-form.

6. Optimization Problem

The optimization problem consists on the determination of the generator sizes minimizing its mass and the power train losses, while respecting the technological constraints of the application.

The generator weight is expressed as follows:

$$W_m = W_{sy} + W_t + W_c + W_{ry} + W_m \quad (21)$$

For the axial flux configurations the weight of stator yoke W_{sy}, tooth W_t, copper W_c, rotor yoke W_{ry}, and magnets W_m are expressed as follows:

$$W_{sy} = n \times d \frac{\pi}{4} \times \left(D_e^2 - D_i^2 \right) \times t_{sy} \quad (22)$$

$$W_t = n \times d \times N_t \times A_t \times h_s \quad (23)$$

$$W_c = 3 \times n \times N_s \times L_{sp} \times \frac{I_{dim}}{\delta} \times d_c \quad (24)$$

$$W_{ry}=\pi\times\left(\left(\frac{D_e}{2}\right)^2-\left(\frac{D_i}{2}\right)^2\right)\times t_{ry}\times d \quad (25)$$

$$W_m=2\times n\times p\times A_m\times t_m\times d_m \quad (26)$$

where d is the density of the metal sheet, d_c is the density of copper, d_m is the magnet density, A_a is the magnet angular width, A_d is the angular width of principal teeth and A_e is the slot angular width.

For the trapezoidal wave-form configurations, the copper losses are expressed by the following relation:

$$P_c=2\times R\times I^2 \quad (27)$$

The phase resistance is given by the following expression:

$$R=r_{cu}(T_b)\times\frac{N_s\times L_{sp}}{S_c} \quad (28)$$

where r_{cu} is the copper receptivity, L_{sp} is the average length of spire, T_b is the copper temperature and S_c is the active section of one conductor:

$$S_c=\frac{I_{dim}}{\delta} \quad (29)$$

The iron losses are expressed by the following relation [14], [15], [16], [17], [18], [19]:

$$P_{fer}=C\times f^{1.5}\times\left(n\times W_t\times B_g^2+n\times W_{sy}\times B_{sy}^2\right) \quad (30)$$

where c is the core loss, f is the motor supplying frequency, W_t is the teeth weight, W_{sy} is the stator yoke weight, B_g is the ai-rgap flux density and B_{sy} is the flux density in stator yoke. The mechanical losses are expressed by the following relation [11]:

$$P_m=\left(T_b+T_{vb}+T_{fr}\right)\times\Omega \quad (31)$$

where Ω is the angular speed of the electric generator.

The losses in the static converter are nearly hopeless, they are not held in account in the model of power train losses calculation.

$$P_{ptl}=P_c+P_{fer}+P_m \quad (32)$$

7. Genetic Algorithms Optimization of the Generator Mass and the Power Train Losses

The function to optimize is expressed by the following expression:

$$F_o=W_m+a\,P_{ptl} \quad (33)$$

Where "a" is a coefficient fixing the influence degree of P_{ptl} at the global objective function compared to W_m. Indeed, "a" brings closer the value of (a P_{ptl}) to the value of W_m.

The optimization problem consists in optimizing the F_o with respect to the problem constraints. In fact, Genetic Algorithms (GAs) are used to find optimal values of the internal diameter D_i, the external diameter D_e, the flux density in the air-gap B_g, the current density in the coils δ, the flux density in the rotor yoke B_{ry} , the flux density in the stator yoke B_{sy} and the number of phase spires N_s [14], [15], [16], [17], [18], [19].

The beach of variation of each parameter xi ∈ (D_i, D_e, B_g, δ, B_{ry} , B_{sy}, Ns) must respect the following constraint: $x_{imin} \leq x_i \leq x_{imax}$. The values of the lower limit x_{imin} and the upper limit x_{imax} are established following technological, physical and expert considerations.

The F_o model is coupled to a program of optimization by the method of the genetic algorithm. The progress of the program of optimization of the F_o with constraints is described by this organization diagram (figure 3) [14], [15], [16], [17], [18]:

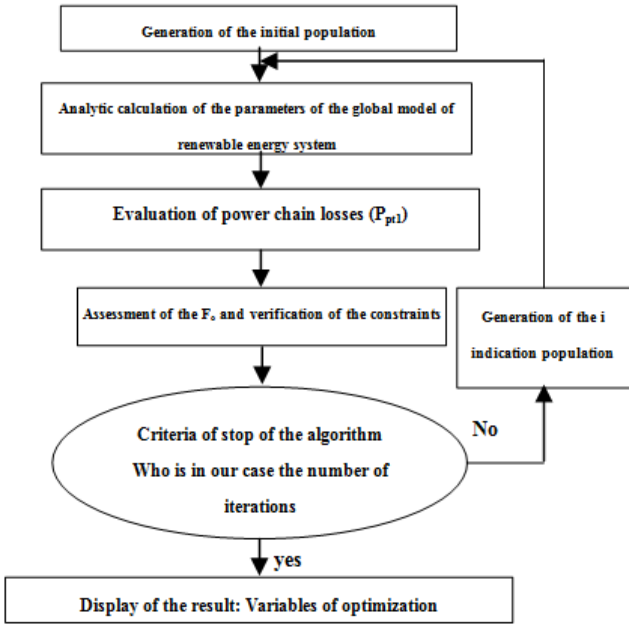

Figure 3. *Progress of the optimization program.*

8. Conclusion

An analytical model dimensioning the renewable energy generator is developed. This model is coupled to an optimization program in order to find the design prameters of the generator minimizing the power train energy losses and the generator cost. This study encourages the manufacture procedure the studied generator [9], [14], [15], [16], [17], [18], [19].

References

[1] Chaithongsuk, S., Nahid-Mobarakeh, B., Caron, J., Takorabet, N., & Meibody-Tabar, F. : Optimal design of permanent magnet motors to improve field-weakening performances in variable speed drives. Industrial Electronics, IEEE Transactions on, vol 59 no 6, p. 2484-2494, 2012.

[2] Rahman, M. A., Osheiba, A. M., Kurihara, K., Jabbar, M. A., Ping, H. W., Wang, K., & Zubayer, H. M. : Advances on single-phase line-start high efficiency interior permanent magnet motors. Industrial Electronics, IEEE Transactions on, vol 59 no 3, p. 1333-1345, 2012.

[3] C.C Hwang, J.J. Chang : Design and analysis of a high power density and high efficiency permanent magnet DC motor, Journal of Magnetism and Magnetic Materials, Volume 209, Number 1, February 2000, pp. 234-236(3)-Publisher: Elsevier.

[4] MI. Chunting CHRIS : Analytical design of permanent-magnet traction-drive motors" Magnetics, IEEE Transactions on Volume 42, Issue 7, July 2006 Page(s):1861 - 1866 Digital Object Dentifier 10.1109/TMAG.2006.874511.

[5] S.TOUNSI, R.NÉJI, F.SELLAMI : Conception d'un actionneur à aimants permanents pour véhicules électriques, Revue Internationale de Génie Électrique volume 9/6 2006 - pp.693-718.

[6] Sid Ali. RANDI : Conception systématique de chaînes de traction synchrones pour véhicule électrique à large gamme de vitesse. Thèse de Doctorat 2003, Institut National Polytechnique de Toulouse, UMRCNRS N° 5828.

[7] C. PERTUZA : Contribution à la définition de moteurs à aimants permanents pour un véhicule électrique routier. Thèse de docteur de l'Institut National Polytechnique de Toulouse, Février 1996.

[8] S. TounsI, R. NEJI and F. SELLAmI: Mathematical model of the electric vehicle autonomy. ICEM2006 (16th International Conference on Electrical Machines), 2-5 September 2006 Chania-Greece, CD: PTM4-1.

[9] R. NEJI, S. TOUNSI, F. SELLAMI: Contribution to the definition of a permanent magnet motor with reduced production cost for the electrical vehicle propulsion. Journal European Transactions on Electrical Power (ETEP), Volume 16, issue 4, 2006, pp. 437-460.

[10] P. BASTIANI : Stratégies de commande minimisant les pertes d'un ensemble convertisseur machine alternative : application à la traction électrique. Thèse INSA 01 ISAL 0007, 2001.

[11] G. Henriot : Traité théorique et pratique des engrenages : théorie et technologie 1. tome 1 Edition Dunod 1952.

[12] D-H. Cho, J-K. Kim, H-K. Jung and C-G. Lee: Optimal design of permanent-magnet motor using autotuning Niching Genetic Algorithm, IEEE Transactions on Magnetics, Vol. 39, No. 3, May 2003.

[13] Islam, M. S., Islam, R., & Sebastian, T. : Experimental verification of design techniques of permanent-magnet synchronous motors for low-torque-ripple applications. Industry Applications, IEEE Transactions on, vol 47 no 1, p. 88-95, 2011.

[14] Parasiliti, F., Villani, M., Lucidi, S., & Rinaldi, F. : Finite-element-based multiobjective design optimization procedure of interior permanent magnet synchronous motors for wide constant-power region operation. Industrial Electronics, IEEE Transactions on, vol 59 no 6, p. 2503-2514, 2012.

[15] Mahmoudi, A., Kahourzade, S., Rahim, N. A., & Ping, H. W. : Improvement to performance of solid-rotor-ringed line-start axial-flux permanent-magnet motor. Progress In Electromagnetics Research, 124, p. 383-404, 2012.

[16] Duan, Y., & Ionel, D. M. : A review of recent developments in electrical machine design optimization methods with a permanent-magnet synchronous motor benchmark study. Industry Applications, IEEE Transactions on, vol 49 no 3, p. 1268-1275, 2013.

[17] Liu, G., Yang, J., Zhao, W., Ji, J., Chen, Q., & Gong, W. : Design and analysis of a new fault-tolerant permanent-magnet vernier machine for electric vehicles. Magnetics, IEEE Transactions on, vol 48 no 11, p. 4176-4179, 2012.

[18] Lee, S., Kim, K., Cho, S., Jang, J., Lee, T., & Hong, J. : Optimal design of interior permanent magnet synchronous motor considering the manufacturing tolerances using Taguchi robust design. Electric Power Applications, IET, vol 8 no 1, 23-28, 2014.

[19] TOUNSI, R. NEJI and F. SELLAMI : Electric vehicle control maximizing the autonomy : 3rd International Conference on Systems, Signal & Devices (SSD'05), SSD-PES 102, 21-24 March 2005, Sousse, Tunisia.